CDF note 8405

Search for Gluino and Squark Production in Multijets plus missing $\mathrm{E_T}$ Final States

The CDF Collaboration
URL http://www-cdf.fnal.gov
(Dated: July 24, 2006)

We present preliminary results on the search for squark and gluino production in proton-antiproton collisions at $\sqrt{s} = 1.96$ TeV using 371 pb^{-1} of CDF Run II data. Events with multiple jets of hadrons and large missing transverse energy in the final state are studied within mSUGRA framework and assuming R-parity conservation. No excess with respect to Standard Model predictions is observed. In a mSUGRA scenario with $A_0 = 0$, $\mu < 0$ and $\tan\beta = 5$, we exclude masses up to 387 $\mathrm{GeV/c^2}$ at 95% C.L. in the region where gluino and squark masses are similar.

I. INTRODUCTION

The search for supersymmetry (SUSY) [1] constitutes one of the pillars of the physics program that explores the energy frontier at the Tevatron. SUSY provides an attractive solution to the hierarchy problem in the Standard Model (SM), further supported by the observation that, within SUSY framework, unification of forces could be accomplished at the GUT scale. In a gravity mediated SUSY breaking scenario, minimal supergravity (mSUGRA), and assuming unification of masses and couplings at the GUT scale, the *a priori* vast SUSY parameter space is reduced to only five parameters that completely determine the phenomenology of the model, and can be explored experimentally: the common scalar mass (m_0), the common gaugino mass ($m_{1/2}$), the common soft trilinear SUSY breaking parameter A_0, the ratio of the Higgs vacuum expectation values at the electroweak scale ($\tan\beta$) and the sign of the Higgsino mass term (sign $\mu = \pm 1$). When R-parity is imposed to be conserved, in order to explicitly preserve conservation of leptonic and baryonic numbers, each interaction vertex must involve an even number of SUSY particles and the lightest supersymmetric particle (LSP) in the spectrum, usually nominated as the lightest neutralino $\tilde{\chi}_1^0$, becomes stable. As a result, SUSY particles must be produced in pairs and a very distinctive signature of large missing transverse energy, $\not\!\!E_T$, from the presence of $\tilde{\chi}_1^0$s, should be observed in the experiment.

The inclusive production of gluino and squark constitutes one of the most promising channels for the discovery of SUSY at colliders, thanks to the strong couplings involved. The cascade decays of squarks and gluinos into quarks and gluons produce multiple jets of hadrons in the final state together with large missing transverse energy from $\tilde{\chi}_1^0$s at the end of the decay process. In this letter, we report preliminary results on the search for squark and gluino production in $p\bar{p}$ collisions at $\sqrt{s} = 1.96$ TeV in events with multiple jets and missing transverse energy in the final state, using 371 pb^{-1} of data collected by the CDF experiment in Run II.

II. MONTE CARLO SIMULATION

A. mSUGRA

In this study, a mSUGRA scenario ($M_{\tilde{q}} \gtrsim M_{\tilde{g}}$) [2] with $A_0 = 0$, sign(μ)=-1 and $\tan\beta = 5$ is assumed. The gluino/squark mass plane is scanned via variations of m_0 and $m_{1/2}$ parameters. PYTHIA Monte Carlo [3] is used to generate the different mSUGRA samples with CTEQ5L PDFs, and initial-state gluon radiation and underlying event settings as determined by TUNE A (see Figure 1). In addition, 2-to-2 hard processes involving stop and sbottom production are excluded. The different subprocesses are separately normalized to NLO predictions as determined by PROSPINO [4] with renormalization scale set to the relevant mass according to the final-sate process: $M_{\tilde{g}}$ in gluino pair production, $M_{\tilde{q}}$ in squark pair production, and $\frac{M_{\tilde{q}}+M_{\tilde{g}}}{2}$ in squark/gluino production.

B. Standard Model Processes

Samples of Standard Model processes consistent with multiple jets plus $\not\!\!E_T$ final states topologies have been generated using different Monte Carlo programs. QCD multijet production events, where large $\not\!\!E_T$ comes from partially reconstructed jets in the final state, were generated using PYTHIA TUNE A and CTEQ5L PDFs. The normalization of the QCD samples was determined directly from data in a region with limited $\not\!\!E_T$ and then extrapolated to the region of interest. W+jets and Z+jets events, where large $\not\!\!E_T$ is originated by partially reconstructed jets and/or the presence of neutrinos and muons in the final state, were generated using ALPGEN [5] interfaced to HERWIG [6] and normalized using NLO cross sections as determined by MCFM [7], where the renormalization scale is set to the mass of the relevant weak boson. Similarly, diboson final states were generated using PYTHIA and normalized according to MCFM predictions. Finally, $t\bar{t}$ production events were generated using HERWIG and normalized to the NLO theoretical cross section [8].

The generated samples were passed through a full CDF detector simulation and then reconstructed and analyzed using the same analysis chain as in the data.

III. EVENT SELECTION

The analysis presented in the letter corresponds to a total integrated luminosity of 371 pb^{-1} of data collected by the CDF experiment in Run II. The CDF detector is described in detail in [9]. Events were selected *online* using a three-level trigger path based on the measured energy deposits in the calorimeter towers. In the first-level trigger,

$\not\!\!E_T$> 25 GeV is required. In the second-level trigger, events containing two hardware-based calorimeter clusters with $E_{\rm T}$ > 10 GeV are selected. In the third-level trigger, $\not\!\!E_T$> 35 GeV is required. Offline, jets are reconstructed from the energy deposits in the calorimeter towers using the Run I cone algorithm [10] with $R = 0.7$. The following selection criteria has been imposed:

- The events are selected to have at least one reconstructed primary vertex with z-position within 60 cm around the nominal interaction point.
- Events are required to have at least three jets with $\mathrm{E_T^{jet}} > 25$ GeV and $|\eta^{\rm jet}| < 2.0$, where at least one of the jets in required to be central ($|\eta^{\rm jet}| < 1.1$).
- $\not\!\!E_T$> 70 GeV.
- In order to remove beam-related backgrounds and cosmics rays, the events are required to fulfill
  - EEMF = $\frac{\sum_{\rm jets} E_T^{\rm jet} \cdot f_{\rm emf}^{\rm jet}}{\sum_{\rm jets} E_T^{\rm jet}} > 0.15$, where $f_{\rm emf}^{\rm jet}$ denotes the jet electromagnetic fraction, and the sum runs over the three leading jets in the event. This removes events with large energy deposits in the hadronic section of the calorimeter towers, incompatible with jets from the interaction point.
  - ECHF = $\frac{1}{N_{\rm jets}} \sum_{\rm jets} \frac{\sum_{\rm tracks} P_T^{\rm track}}{E_T^{\rm jet}}$, where $P_T^{\rm track}$ denotes the scalar sum of the momentum of the tracks inside the jet cone and the sum runs over jets with $|\eta^{\rm jets}| < 1.1$. This cut removes events where the activity in the central calorimeter is incompatible with that in the central tracker.

Additional selection criteria are applied to suppress the different SM background contributions:

- A cut on the azimuthal distance between the $\not\!\!E_T$ direction and each of the three jets, $\Delta\phi(\mathrm{jet} - \not\!\!E_{\rm T}) > 0.7$, is applied to reduce the QCD multijet contribution.
- Background from W and Z production with misidentified electrons as jets is suppressed by requiring that the electromagnetic fraction of each of the three leading jets is smaller that 0.9.
- Background from Z and W production with high-p_t muons in the final state are identified via the the presence of isolated tracks. $Z \to \mu\mu$ background is reduced by requiring that the invariant mass of the two highest p_t isolated tracks lies outside the $76 < M_{\rm inv} < 106$ GeV/c^{2}mass window. Remaining Z and W background is further reduced by requiring that the direction of the highest p_t isolated track in the transverse plane should not be aligned with the $\not\!\!E_T$, $\Delta\phi(\mathrm{track} - \not\!\!E_{\rm T}) > 0.7$.

A dedicated study was carried to define the selection criteria that optimize the sensitivity to mSUGRA signals. The study was based on four different, but highly correlated, variables: $\not\!\!E_T$, the $\mathrm{E_T}$ of the three leading jets, and H_T=$\sum_1^3 E_T^{\rm jet}$. A $S/\sqrt{B}$ optimization, where S denotes the signal and B the background number of events, was performed in different regions of the squark/gluino mass plane. Three different set of thresholds, intended for different gluino masses, were defined in order to increase the signal significance across the plane (see Figure 1 and Table I).

	$\not\!\!E_{\rm T}$ (GeV)	$\mathrm{H_T}$ (GeV)	$\mathrm{E_T^{jet\,1}}$ (GeV)	$\mathrm{E_T^{jet\,2}}$ (GeV)	$\mathrm{E_T^{jet\,3}}$ (GeV)
Set A	75	230	95	55	25
Set B	90	280	120	70	25
Set C	120	330	140	100	25

TABLE I: Different set of thresholds employed in this analysis.

IV. SYSTEMATIC UNCERTAINTIES

A detailed study of systematic uncertainties was carried out [11] for SM background yields and mSUGRA signal efficiencies separately for each set of optimized cuts. The uncertainty on the SM background estimation is dominated by a ±3% uncertainty on the absolute jet energy scale that translates into a uncertainty between ±15% and ±30% on the background yields. It is followed by contributions related to uncertainties on the PDFs and renormalization scale (±12%), and total integrated luminosity (±6%). The uncertainty on the mSUGRA signal efficiencies is dominated by

the uncertainty on the absolute jet energy scale and varies between ±7% and ±10% with increasing gluino and squark masses. It is followed by the uncertainty on the modeling of initial- and final-state gluon radiation in the mSUGRA samples which introduces an about ±5% uncertainty on the the signal efficiencies.

The systematic uncertainty on the mSUGRA signal cross sections itself was also studied. It is dominated by a ±30% contribution related to the uncertainty on the PDFs, as determined using the hessian method [12], and followed by a ±20% uncertainty from factor 2 variations on the renormalization scale in PROSPINO.

V. RESULTS

Table II shows the total number of events in the data and the SM expectations, corresponding to a total integrated luminosity of 371 pb^{-1}, for the different set of thresholds considered in the analysis. In all cases, the SM Monte Carlo predictions provide a reasonable description of the data and no excess with respect to the SM is observed. Figures 2 to 4 present the measured $\not\!\!E_T$ and H_T distributions for the three set of cuts compared to the different SM contributions and the signal for a representative mSUGRA point. The Figures show the data after all cuts are applied expect the one on the distribution considered.

	Set A	Set B	Set C
Observed data	185	40	2
Expected SM background	211 ± 7(stat.) ± 44(syst.)	56 ± 3(stat.) ± 14(syst.)	8.2 ± 1.2(stat.) ± 2.6(sys.)

TABLE II: Total number of events observed in the data compared to SM background predictions for the different set of cuts employed in the analysis.

The results are translated into exclusion limits at 95% C.L. on gluino and squark production as a function of squark and gluino masses using a Bayesian approach, where correlations between systematic uncertainties on signal and background are properly taken into account. In addition, theoretical uncertainties on the signal cross sections were input to the Bayesian limit calculation. This differs from the more conservative approach adopted by the *DØ* Collaboration [13]. As a result, in this analysis limits on squark and gluino masses are determined from the crossing points between the obtained observed limits and the nominal PROSPINO cross sections. As an example, Figure 5 shows the theoretical cross sections as a function of the average squark mass for fixed gluino masses at 235 and 255 GeV/c^2, respectively, overlaid with the observed and expected 95% C.L. curves. Figure 6 shows the theoretical cross section as a function of the gluino mass, in the region where squark and gluino masses are similar, compared to the corresponding observed and expected 95% C.L. curves. The obtained limits from the different quark and gluino masses are mapped out in Figure 7, together with previous results. From the analysis presented in this letter, in the region where $M_{\tilde{g}} \approx M_{\tilde{q}}$, we exclude squark and gluino masses up to ≈ 387 GeV/c^2 at 95% C.L.

Acknowledgments

We thank the Fermilab staff and the technical staffs of the participating institutions for their vital contributions. This work was supported by the U.S . Department of Energy and National Science Foundation; the Italian Istituto Nazionale di Fisica Nucleare; the Ministry of Education, Culture, Sports, S cience and Technology of Japan; the Natural Sciences and Engineering Research Council of Canada; the National Science Council of the Republic of China; the Swiss National Science Foundation; the A.P. Sloan Foundation; the Bundesministerium fuer Bildung und Forschung, Germany; the Korean Science and Engi neering Foundation and the Korean Research Foundation; the Particle Physics and Astronomy Research Council and the Royal Society, UK; the Russian Founda tion for Basic Research; the Comision Interministerial de Ciencia y Tecnologia, Spain; in part by the European Community's Human Potential Programme und er contract HPRN-CT-2002-00292; and the Academy of Finland.

[1] For a review on SUSY see: H.-P. Nilles, Phys. Rept. **110**, 1 (1984).
[2] In this letter $M_{\tilde{q}}$ denotes the average over 8 squarks and anti-squaks from the first two generations.
[3] T. Sjöstrand *et al.*, Comp. Phys. Comm. **135**, 238 (2001).
[4] W. Beenakker , R. Hopker , M. Spira , P.M. Zerwas, Nucl. Phys. B **492** 51 (1997).
[5] M.L. Mangano, M. Moretti, F. Piccinini, R. Pittau, A. Polosa, JHEP 0307:001,2003.

[6] G. Corcella *et al.*, JHEP **0101**, 010 (2001).
[7] John Campbell, R.K. Ellis, Phys. Rev. D **65** 113007 (2002).
[8] M. Cacciari, et al., JHEP 0404:068 (2004).
[9] D. Acosta *et al.* (CDF Collaboration), Phys. Rev. D **71**, 032001 (2005).
[10] CDF Collab., F. Abe et al.,Phys. Rev. D **45**, 1448 (1992).
[11] Xavier Portell, PhD. Thesis, Universitat Autónoma de Barcelona, in preparation.
[12] J. Pumplin *et al.*, Phys. Rev. D **65**, 014013 (2002).
[13] DO Collaboration, V. Abazov, et al., Phys. Lett. B **638**, 119-127 (2006).
[14] UA1 Collaboration, C. Albajar *et al.*, Phys. Lett. **B198** (1987) 261.
[15] UA2 Collaboration, S. Albachi *et al.*, Phys. Lett. **B235** (1990) 363.
[16] DO Collaboration, B. Abbott *et al.*, Phys. Rev. Lett. **83** (1999) 4937.
CDF Collaboration, T. Affolder *et al.*, Phys. Rev. Lett. **88** (2002) 041801.
[17] The LEP-SUSY working group: *http://lepsusy.web.cern.ch/lepsusy/*

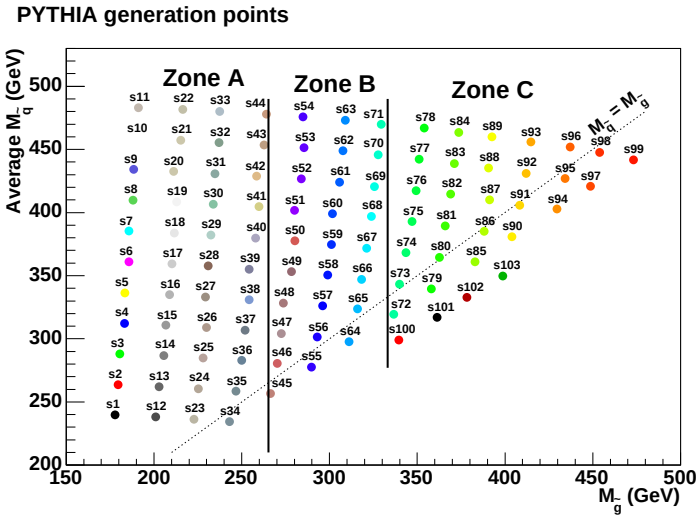

FIG. 1: mSUGRA points generated in the squark/gluino mass plane. The vertical lines denote the zones defined during optimization process, as described in section III.

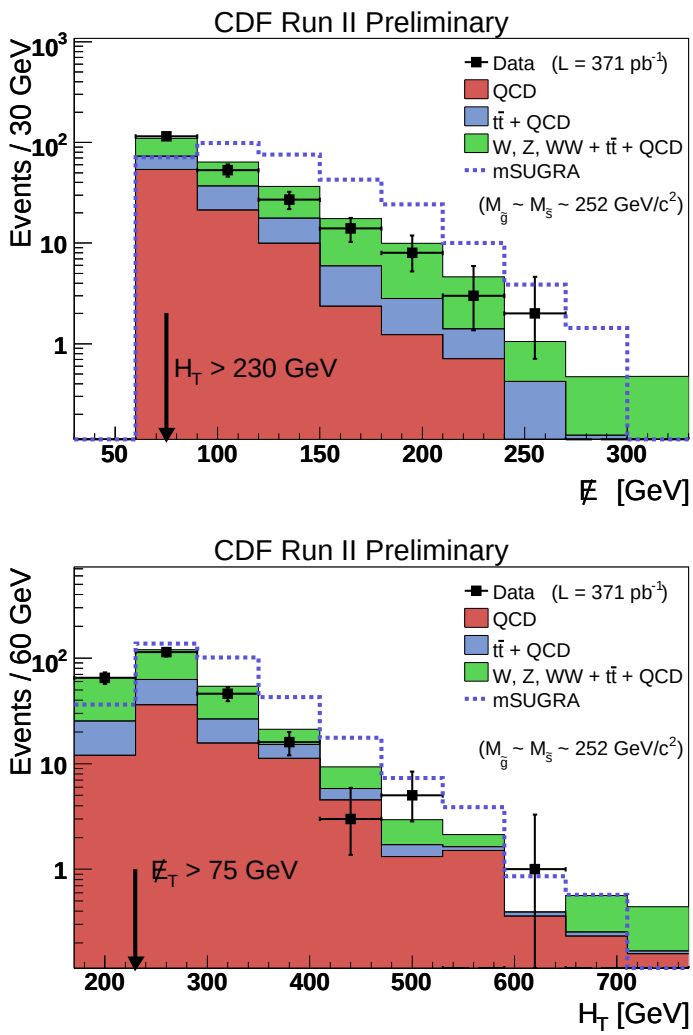

FIG. 2: Measured $\not{E}_T$ and H_T distributions (black dots) after all set A cuts but the one on the distribution (shown by the arrow), compared to the SM (filled histograms). For illustration, a representative mSUGRA point is included (dashed histogram).

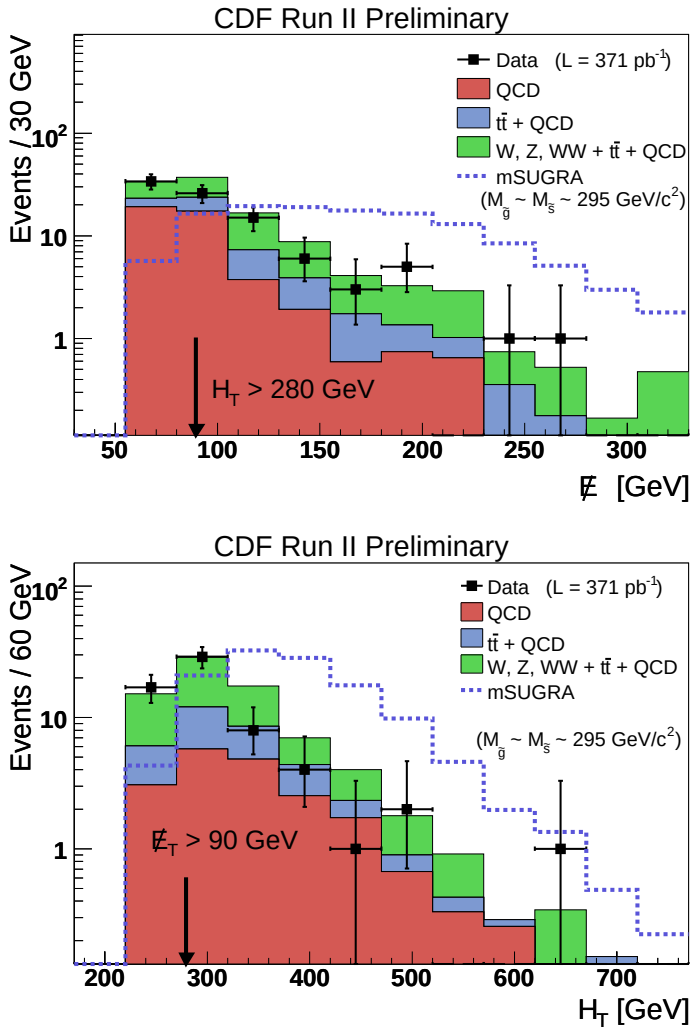

FIG. 3: Measured $\not{E}_T$ and H_T distributions (black dots) after all set B cuts but the one on the distribution (shown by the arrow), compared to the SM (filled histograms). For illustration, a representative mSUGRA point is included (dashed histogram).

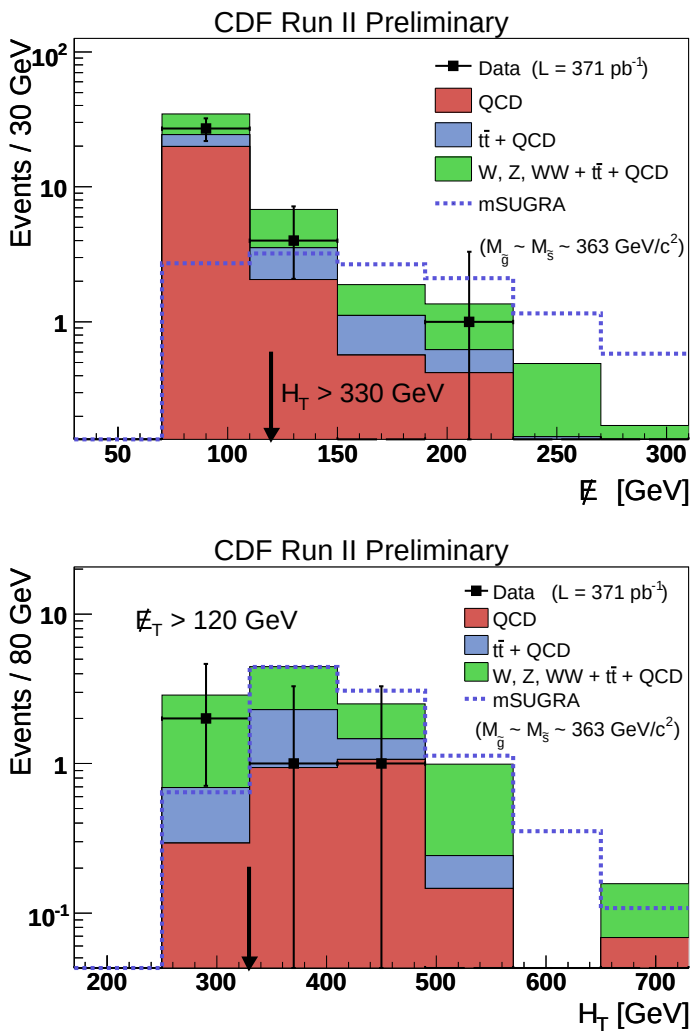

FIG. 4: Measured $\not{E}_T$ and H_T distributions (black dots) after all set C cuts but the one on the distribution (shown by the arrow), compared to the SM (filled histograms). For illustration, a representative mSUGRA point is included (dashed histogram).

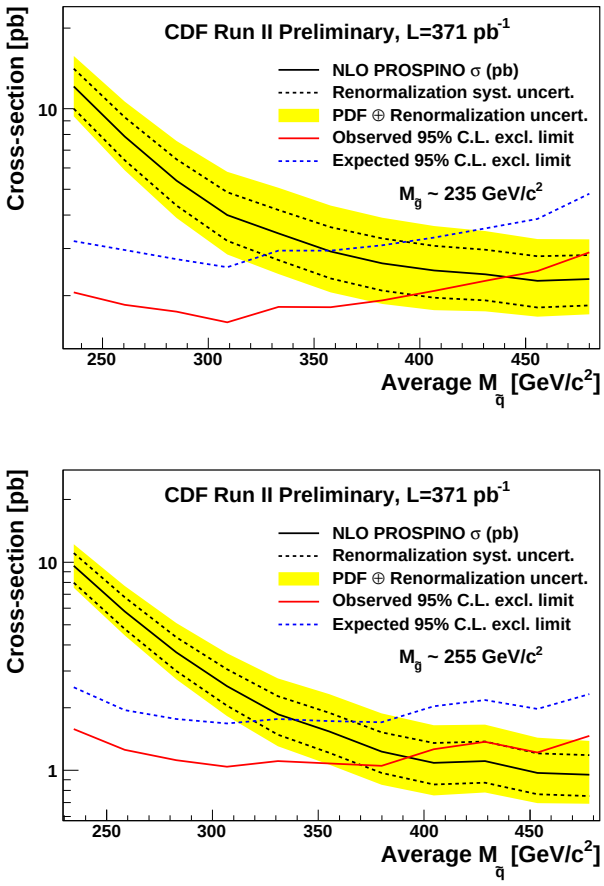

FIG. 5: PROSPINO cross section as a function of $M_{\tilde{q}}$ for $M_{\tilde{g}}$ equal to 235 and 255 GeV/c^2. The yellow band shows the total systematic uncertainty on the theoretical prediction. The observed and expected limits at 95% C.L., as extracted from this analysis, are also shown.

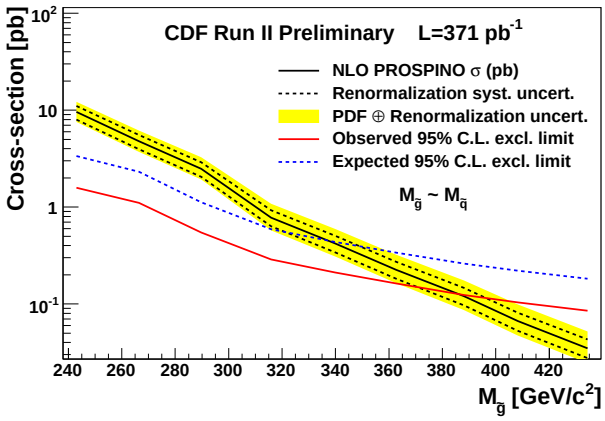

FIG. 6: PROSPINO cross section as a function of $M_{\tilde{g}}$ for $M_{\tilde{q}} \approx M_{\tilde{g}}$. The yellow band shows the total systematic uncertainty on the theoretical prediction. The observed and expected limits at 95% C.L., as extracted from this analysis, are also shown.

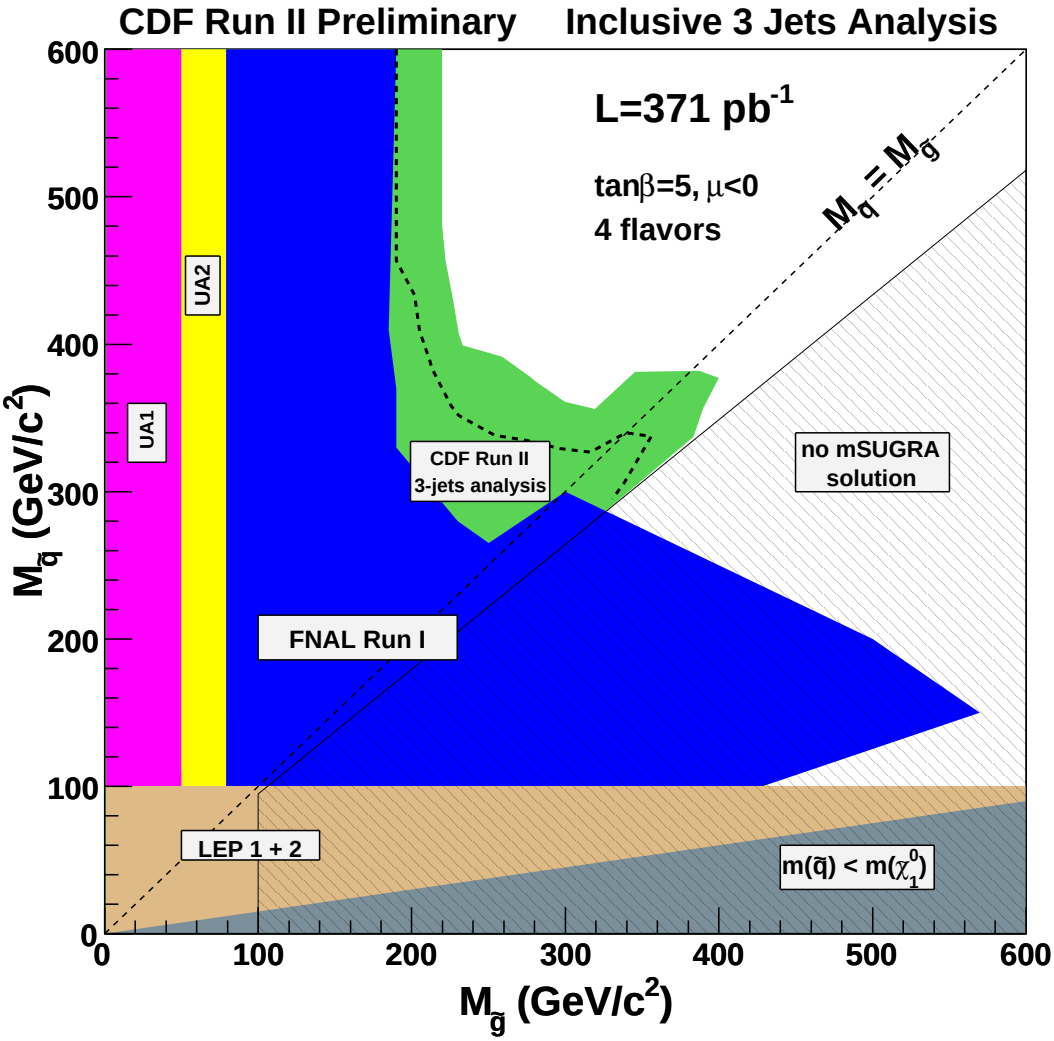

FIG. 7: $M_{\tilde{q}}$ - $M_{\tilde{g}}$ exclusion plot at the 95 % C.L in the framework of mSUGRA and assuming R-parity conservation. The pink region is excluded by the UA1 experiment [14]. The yellow region is excluded by the UA2 experiment [15]. The blue region is excluded by the CDF and DØ Run I [16] results. The brown region is excluded by the LEP experiment [17]. In the bottom gray region, the squark mass is smaller than the mass of the lightest neutralino. In the black hashed region, there is no mSUGRA solution. The green region shows the area excluded by this analysis.